

Aerodynamics of Two Side-by-Side Plates in Hypersonic Rarefied-Gas Flows

Vladimir V. Riabov*

Rivier College, Nashua, New Hampshire 03060

Hypersonic rarefied-gas flows near two side-by-side plates have been studied numerically with the direct simulation Monte Carlo technique under transitional rarefied-gas-flow conditions (Knudsen numbers from 0.024 to 1.8). Strong influences of the geometrical factor (ratio of distance between plates to plate length) and the Knudsen number on the flow structure (the shape of shock waves, the configuration of subsonic flow zones), skin friction, pressure distribution, lift, and drag have been found. For small geometrical factors, the repulsive lift force becomes significant with a lift-drag ratio of 1.7 for near-continuum flow, but decreases significantly (0.4) in the near-free-molecular flow. Results show that the lift, drag, and lift-drag ratio dependency on the Knudsen number is nonmonotonic for various geometrical factors.

Nomenclature

A	=	plate area, $L \times 1$, m ²
C_f	=	local skin-friction coefficient, τ_w/qA
C_p	=	local pressure coefficient, $(p_w - p_\infty)/qA$
C_x	=	drag coefficient
C_y	=	lift coefficient
H	=	distance between the plane of symmetry and the plate inside surface, m
h	=	plate thickness, 0.01 m
$Kn_{\infty,L}$	=	Knudsen number
L	=	plate length, 0.1 m
M	=	Mach number
p	=	pressure, N/m ²
q_∞	=	dynamic pressure, $0.5 \rho_\infty u_\infty^2$, N/m ²
δ	=	dimensionless plate thickness, h/L
τ_w	=	viscous stress at the plate surface, N/m ²

Subscripts

FM	=	free-molecular-flow parameter
L	=	plate length as a length-scale parameter
w	=	wall condition
∞	=	freestream parameter

Introduction

NUMERICAL and experimental studies^{1–5} of aerothermodynamics of simple shape bodies have provided valuable information related to physics of hypersonic flows about spacecraft elements and testing devices. Numerous results have been found in the cases of plates, wedges, cones, disks, spheres, torus, and cylinders.^{1–8} The interference effect for cylinder grids and flat strips was experimentally studied by Coudeville et al.⁹ for transition rarefied-gas flows.

Supersonic, subsonic, and pressure-driven, low-speed flows in two-dimensional microchannels of varying aspect ratios, $20 \geq L/2H \geq 2.5$, were studied with the direct simulation Monte Carlo (DSMC) technique by Mavriplis et al.¹⁰ and Oh et al.¹¹ for a range of continuum to transition rarefied-gas flow regimes. The results^{10,11} were in qualitative agreement with other computational

and experimental results for longer microchannels. Near the continuum limit, they show the same trends as classical theories,¹⁰ such as Fanno/Rayleigh flow and boundary-layer interaction with shocks.

In the present study, the hypersonic rarefied-gas flow about two side-by-side plates of varying small aspect ratios, $2 \geq L/2H \geq 0.4$, has been studied. The flow pattern for such a configuration has not been discussed in the research literature. Several features of the flow are unique. For example, if the distance between the plates, $2H$, is significantly larger than the plate length L , then the flow can be approximated by a stream between two isolated plates.^{3–7} At $H \leq 0.25L$, the rarefied-gas flow has some features of a stream near a bluff body.¹² In the first case, two oblique shock waves would interact in the vicinity of the symmetry plane generating the normal shock wave and the Mach reflected waves far behind the bodies. In the second case, the front shock wave would be normal, and the pressure and skin-friction distributions along the upper and bottom surfaces would be difficult to predict. At $H \leq 0.5L$, the flow pattern and shock-wave shapes are very complex. As a result, simple approximation techniques should not be used to define the aerothermodynamics of side-by-side bodies.

In the present study, the argon flow about two side-by-side plates and their aerodynamic characteristics have been studied under the conditions of a hypersonic rarefied-gas stream at Knudsen numbers $Kn_{\infty,L}$ from 0.024 to 1.8 and a range of geometrical factors ($1.25L \geq H \geq 0.25L$). The numerical results have been obtained using the DSMC technique.³ The computer code¹³ was developed by Bird.

DSMC Simulation

The DSMC method³ has been used in this study as a numerical simulation technique for low-density hypersonic-gas flows. A two-dimensional DSMC code¹³ (the latest version 3.2 of the DS2G program) is used in this study. Molecular collisions in argon and air are modeled using the variable hard sphere (VHS) molecular model.³ The gas-surface interactions are assumed to be fully diffusive with full moment and energy accommodation.

Code validation was established³ by comparing numerical results with experimental data^{4,5} related to simple-shape bodies, including plates. As an example, the comparison of the DSMC recent numerical results with experimental data⁴ in air is shown in Fig. 1 for a wide range of Knudsen numbers from 0.02 to 3.2 and flow parameters $M_\infty = 10$, $\gamma = 1.4$, and $t_w = 1$. The error of experimental data⁴ (error bars in Fig. 1) was estimated as 8–12% at different flow regimes (see Ref. 4 and the bibliography in Ref. 5). The numerical results correlate well with experimental data at $0.02 < Kn_{\infty,L} < 1$ and approach the free-molecular limit¹⁴ at $Kn_{\infty,L} > 3$.

The methodology from Refs. 3, 10, and 13 has been applied in computations. The cases that had been considered by

Received 31 October 2001; revision received 31 May 2002; accepted for publication 6 June 2002. Copyright © 2002 by Vladimir V. Riabov. Published by the American Institute of Aeronautics and Astronautics, Inc., with permission. Copies of this paper may be made for personal or internal use, on condition that the copier pay the \$10.00 per-copy fee to the Copyright Clearance Center, Inc., 222 Rosewood Drive, Danvers, MA 01923; include the code 0022-4650/02 \$10.00 in correspondence with the CCC.

*Associate Professor, Department of Computer Science and Mathematics, 420 South Main Street. Senior Member AIAA.

Mavriplis et al.¹⁰ for airflows in near-continuum, transitional, and near-free-molecular regimes were reproduced in this study.

The mesh size and the number of molecules per cell were varied until independence of the flow profiles and aerodynamic characteristics from these parameters was achieved for each case. Table 1 shows the DSMC results for the drag coefficient of the plate C_x in the airflow at $Kn_{\infty,L} = 0.13$, $M_{\infty} = 10$, $\gamma = 1.4$, $t_w = 1$, and different computational parameters. The uniform grid has covered the symmetrical flow area 0.024×0.021 m near the 0.01×0.001 m plate. The location of the external boundary with the upstream flow conditions is at 0.01 m from the leading edge of the plate. It has been found that the numerical solutions for C_x are independent of the numerical parameters (Table 1).

The similar parameters have been used in the case of two side-by-side plates. As an example, for calculations at $H/L = 1.25$, the total number of cells near a plate (a half-space of the flow segment

between side-by-side plates) is 12,700 in eight zones (Fig. 2), the argon molecules are distributed evenly, and a total number of 139,720 molecules corresponds to an average 11 molecules per cell. Following the recommendations of Refs. 3 and 13, acceptable results are obtained for an average of at least 10 molecules per cell in the most critical region of the flow. The error was pronounced when this number falls below five. The cell geometry has been chosen to minimize the changes in the macroscopic properties (pressure and density) across the individual cell.¹³ In all cases, the usual criterion³ for the time step Δt_m has been realized, $1 \times 10^{-8} \leq \Delta t_m \leq 1 \times 10^{-6}$ s. Under these conditions, aerodynamic coefficients and gasdynamic parameters have become insensitive to the time step. The ratios of the mean separation between collision partners to the local mean free path and the collision time ratio (CTR)¹³ of the time step to the local mean collision time have been well under unity over the flowfield (Fig. 2).

The DS2G program employed time averaging for steady flows.¹³ About 40,000 samples have been studied in the considered cases. The computed results have been stored to the TECPLOT[®] files that have been further analyzed to study whether the DSMC numerical criteria³ are met.

The location of the external boundary with the upstream flow conditions varies from $0.75L$ to $1.5L$. Calculations were carried out on a personal computer with a Pentium[®] III 850-MHz processor. The computing time of each variant was estimated to be approximately 12–60 h.

Table 1 Drag coefficient of a single plate in airflow at $Kn_{\infty,L} = 0.13$, $M_{\infty} = 10$, $\gamma = 1.4$, $t_w = 1$, and different numerical parameters

Number of cells	Number of molecules per cell	Drag coefficient	Time of calculation
12,700	11	0.4524	12 h 28 min
12,700	22	0.4523	21 h 03 min
49,400	11	0.4525	62 h 06 min
203,200	11	0.4526	187 h 11 min

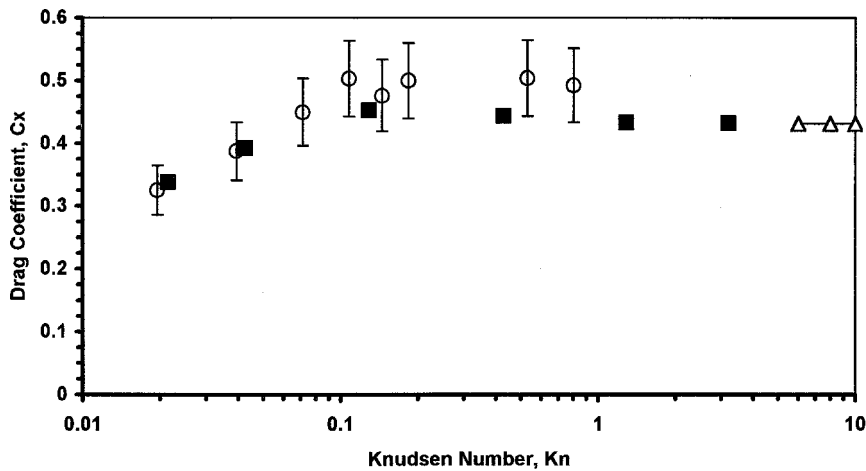


Fig. 1 Total drag coefficient of the plate vs Knudsen number $Kn_{\infty,L}$ in air at $M_{\infty} = 10$: ■, Monte Carlo; ○, experiment (Ref. 4); and △, free-molecular data (Ref. 14).

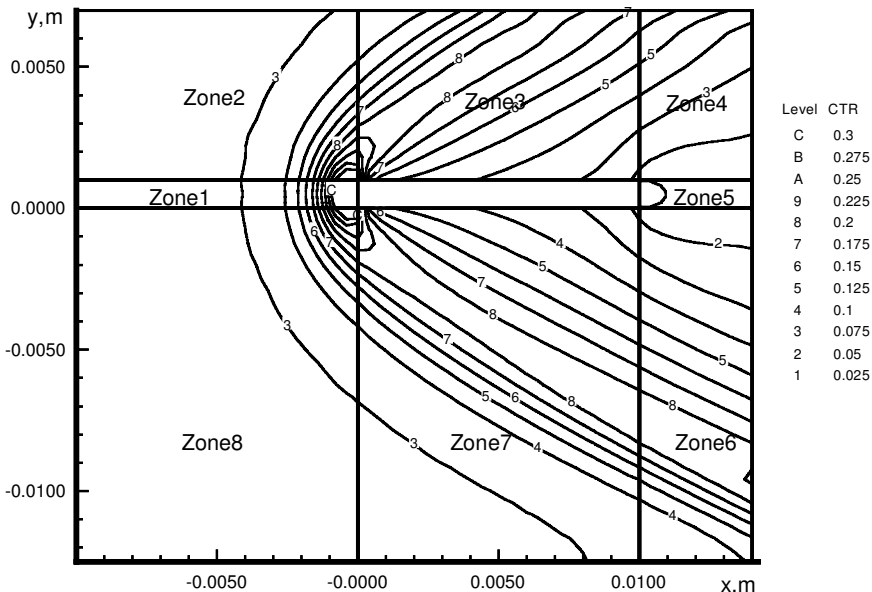


Fig. 2 CTR¹³ of the time step to the local mean collision time in argon flow about a side-by-side plate at $Kn_{\infty,L} = 0.024$ and $H = 1.25L$.

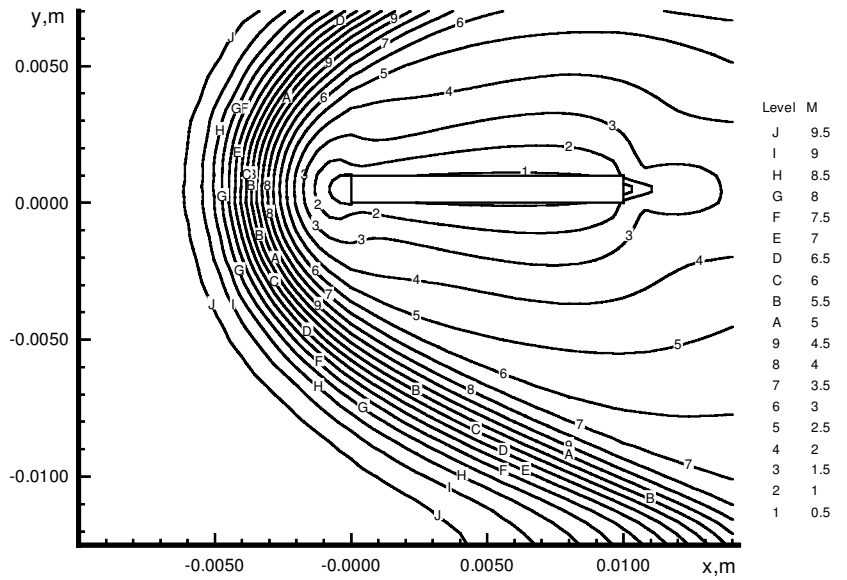


Fig. 3 Mach number contours in argon flow about a side-by-side plate at $Kn_{\infty,L} = 0.024$ and $H = 1.25L$.

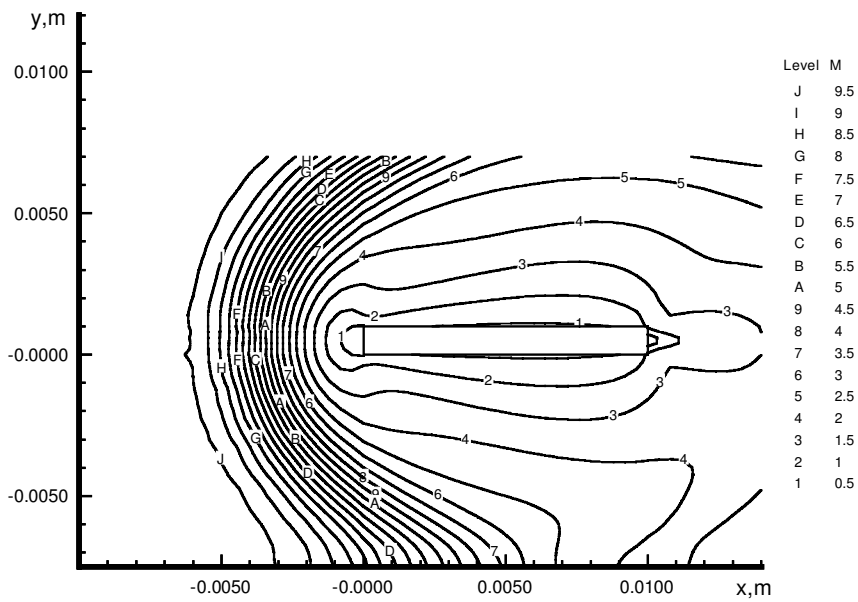


Fig. 4 Mach number contours in argon flow about a side-by-side plate at $Kn_{\infty,L} = 0.024$ and $H = 0.75L$.

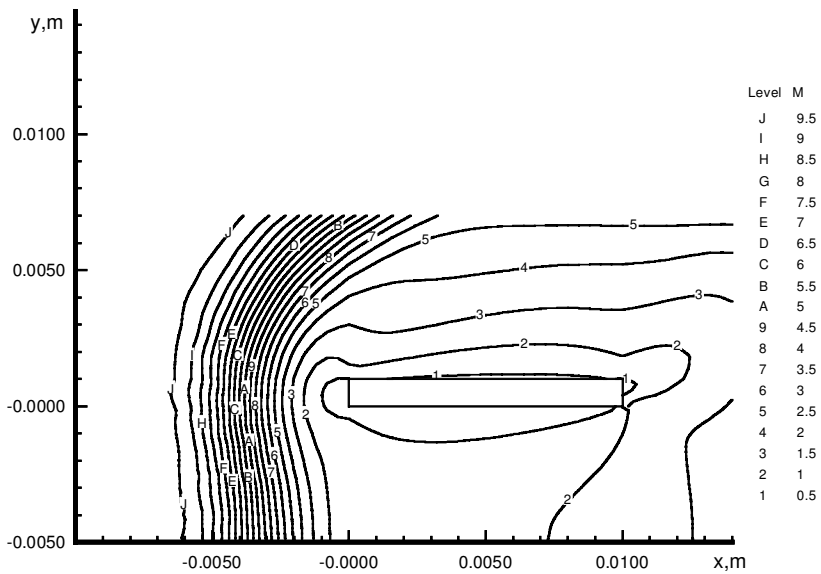


Fig. 5 Mach number contours in argon flow about a side-by-side plate at $Kn_{\infty,L} = 0.024$ and $H = 0.5L$.

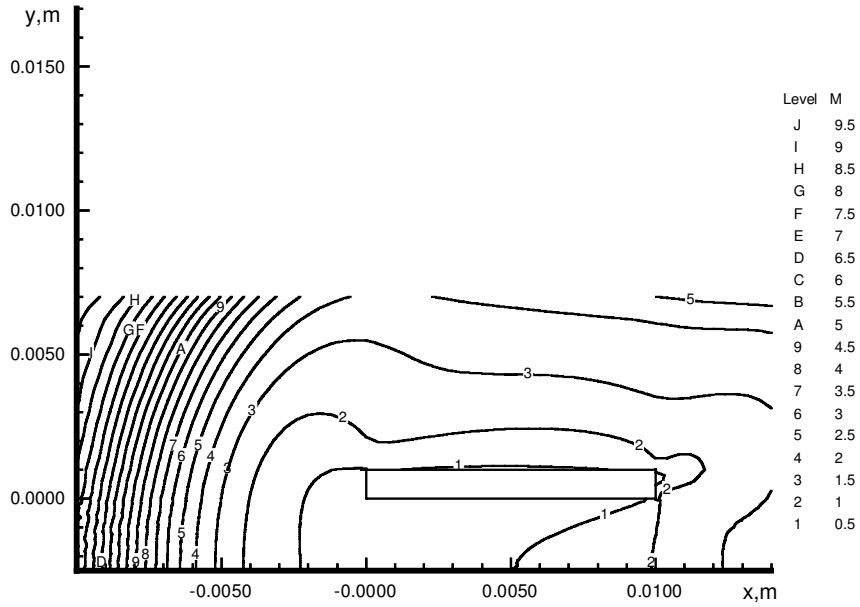


Fig. 6 Mach number contours in argon flow about a side-by-side plate at $Kn_{\infty,L} = 0.024$ and $H = 0.25L$.

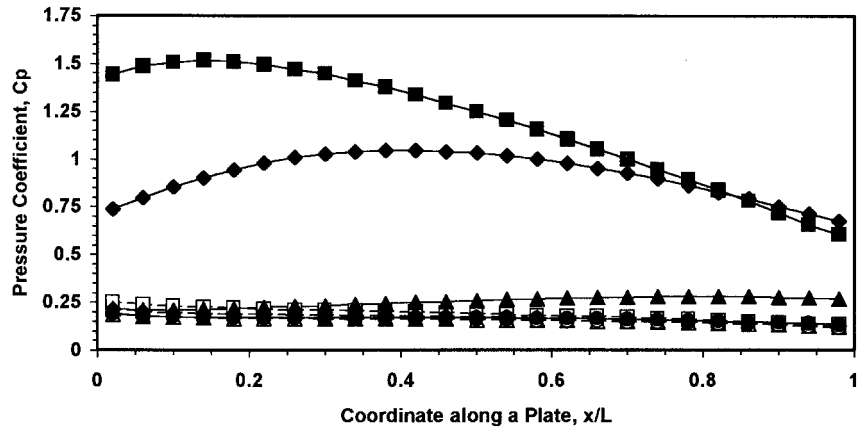


Fig. 7 Pressure coefficient along the side-by-side plate at $Kn_{\infty,L} = 0.07$ and $M_{\infty} = 10$: \square , C_p outside, $H = 0.25L$; \blacksquare , C_p inside, $H = 0.25L$; \diamond , C_p outside, $H = 0.5L$; \blacklozenge , C_p inside, $H = 0.5L$; \triangle , C_p outside, $H = 0.75L$; \blacktriangle , C_p inside, $H = 0.75L$; \circ , C_p outside, $H = 1.25L$; and \bullet , C_p inside, $H = 1.25L$.

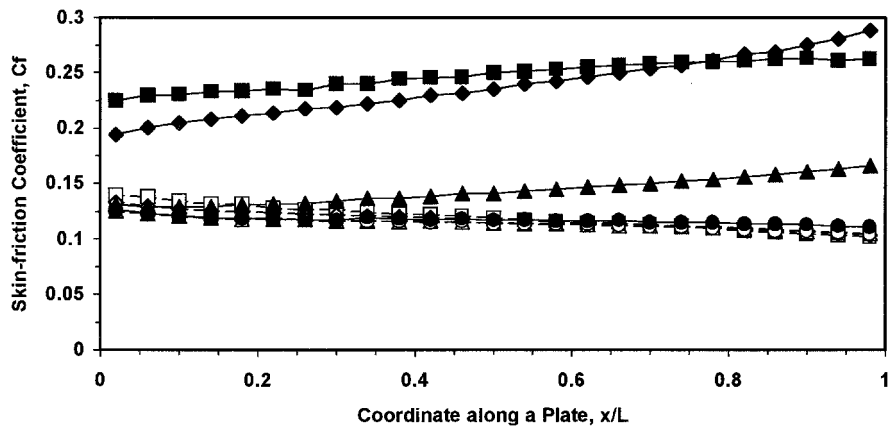


Fig. 8 Skin-friction coefficient along the side-by-side plate at $Kn_{\infty,L} = 0.07$ and $M_{\infty} = 10$: \square , C_f outside, $H = 0.25L$; \blacksquare , C_f inside, $H = 0.25L$; \diamond , C_f outside, $H = 0.5L$; \blacklozenge , C_f inside, $H = 0.5L$; \triangle , C_f outside, $H = 0.75L$; \blacktriangle , C_f inside, $H = 0.75L$; \circ , C_f outside, $H = 1.25L$; and \bullet , C_f inside, $H = 1.25L$.

Results

Influence of the Geometrical Factor, H/L

The flow pattern over two side-by-side plates is significantly sensitive to the major geometrical similarity parameter, H/L . The influence of this parameter on the flow structure has been studied for hypersonic flow of argon at $M_{\infty} = 10$ and $Kn_{\infty,L} = 0.024$. It is assumed that the wall temperature is equal to the stagnation temperature.

The local Mach number contours are shown in Figs. 3–6 for four cases of the geometrical factor ($H/L = 1.25, 0.75, 0.5,$ and 0.25). At $H/L = 1.25$, a strong oblique shock wave can be observed near the plate (Fig. 3). Two oblique shock waves interfere near the symmetry plane. The subsonic and supersonic areas (at $M \leq 2.5$) of the flow near the plates are symmetrical, which indicates that there is no lift force acting on the plates for the specified conditions. At $H/L = 0.75$ (Fig. 4), the subsonic flow zone near the plate

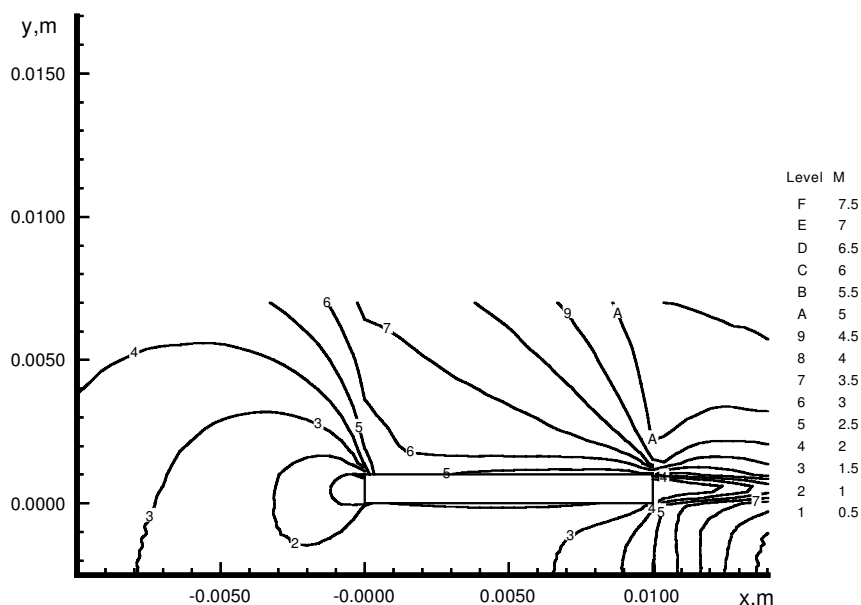


Fig. 9 Mach number contours in argon flow about a side-by-side plate at $Kn_{\infty,L} = 1.8$ and $H = 0.25L$.

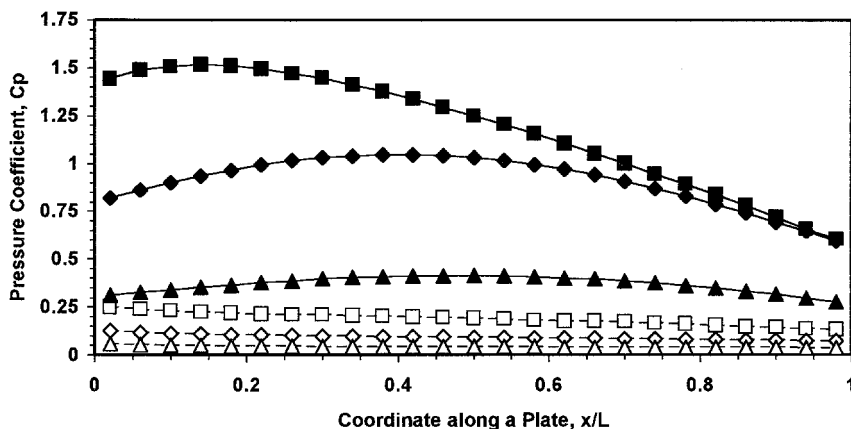


Fig. 10 Pressure coefficient C_p along the side-by-side plate at $H/L = 0.25$ and $M_{\infty} = 10$: \square , C_p outside, $Kn = 0.07$; \blacksquare , C_p inside, $Kn = 0.07$; \diamond , C_p outside, $Kn = 0.24$; \blacklozenge , C_p inside, $Kn = 0.24$; \triangle , C_p outside, $Kn = 0.7$; and \blacktriangle , C_p inside, $Kn = 0.7L$.

becomes slightly asymmetrical, but it is still isolated from the similar zone of the other plate. However, for $H/L \leq 0.5$, the interference of the two plates produces a normal shock wave in the vicinity of the symmetry plane (Figs. 5 and 6). Actually, the whole area of the flow between the two side-by-side plates becomes subsonic. At $H/L = 0.25$ (Fig. 6), the subsonic zone spreads far ahead of the plate leading edge. The effect of the internal subsonic zone is also observed in density, temperature, and velocity contour diagrams. The flow near a plate becoming significantly asymmetrical at $H/L \leq 0.5$ indicates that there is a repulsive lift force acting on the plates under these conditions. The latter effect plays a fundamental role in the redistribution of pressure and skin friction along the plate surface (Figs. 7 and 8, respectively).

The dynamics of the subsonic zone has a major influence on the pressure distributions along the inside surface of the plate. At $0.25 \leq H/L \leq 0.5$, the surface pressure gradient has a negative sign for a significant region of the plate.

Influence of the Knudsen number, $Kn_{\infty,L}$

The rarefaction factor, which can be characterized by the Knudsen number $Kn_{\infty,L}$, plays an important role in the flow structure^{3,5-8,10,11} and aerodynamics.^{1,4,5,8,9} The flowfield about two side-by-side plates has been calculated for hypersonic flow of argon at $M_{\infty} = 10$ and $Kn_{\infty,L} = 0.024, 0.07, 0.24, 0.7$, and 1.8 .

Under near-continuum-flow conditions ($Kn_{\infty,L} = 0.024$), the flow structure has the same features as were discussed earlier. In the transition flow regime, at $Kn_{\infty,L} = 1.8$, the flow pattern is different.

The reflection waves have different shapes and thickness because of the rarefaction effects in the oblique and normal shock waves. The Mach number contours at $H/L = 0.25$ are shown in Fig. 9. The local subsonic zone is located right in front on the blunt plate, with the thickness ratio of 0.1. The outside and inside surfaces of the plate are streamed by supersonic flows at different local Mach numbers.

At a small geometrical factor, $H/L = 0.25$, the pressure and skin-friction coefficient distributions along the plate surfaces become sensitive to the rarefaction parameter $Kn_{\infty,L}$ (Figs. 10 and 11). The pattern of the skin-friction coefficient distributions along the plate is significantly different at various Knudsen numbers.

The calculating results for the total drag and lift coefficients, as well as a lift-drag ratio, are shown in Figs. 12 and 13. At any considered geometrical factor, the results show the drag coefficient to increase with Knudsen number, reach a maximum, and then decrease to the free-molecule value.¹⁴ This fact is in a good agreement with the experimental data of Coudeville et al.⁹ The geometrical factor becomes insignificant as to its influence on the drag as both the continuum- and free-molecule-flow regimes are approached.

As a result of the interference between two side-by-side plates, the repulsive lift force becomes significant at small values of the geometrical factor $H/L \leq 0.5$ and in the transitional flow regimes even at $H/L \leq 0.75$ (Figs. 12 and 13). At small geometrical factors, the repulsive lift force becomes significant with the average lift-drag ratio of 1.6 in the transition regime. The similar effect was discussed by Blevins,¹² who studied viscous incompressible flows

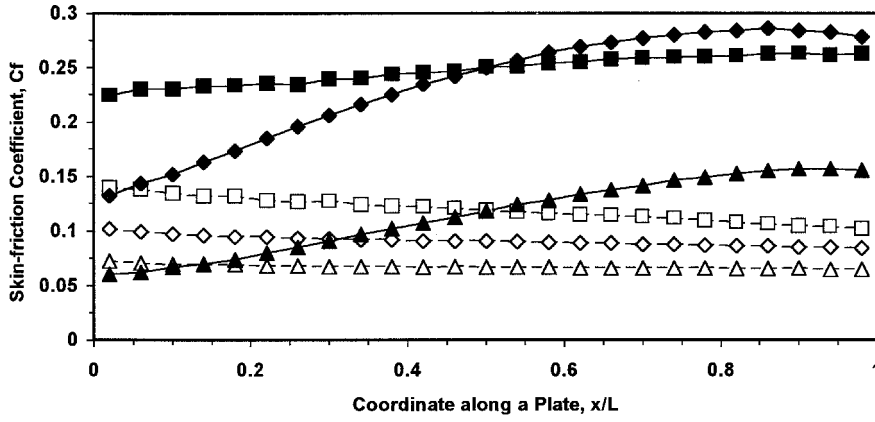


Fig. 11 Skin-friction coefficient C_f along the side-by-side plate at $H/L=0.25$ and $M_\infty=10$: \square , C_f outside, $Kn=0.07$; \blacksquare , C_f inside, $Kn=0.07$; \diamond , C_f outside, $Kn=0.24$; \blacklozenge , C_f inside, $Kn=0.24$; \triangle , C_f outside, $Kn=0.7$; and \blacktriangle , C_f inside, $Kn=0.7L$.

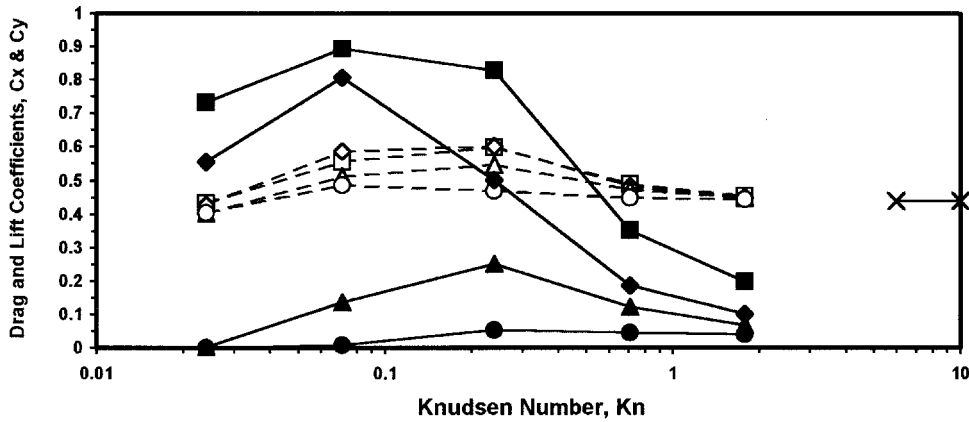


Fig. 12 Total drag and lift coefficients of the side-by-side plate vs Knudsen number $Kn_{\infty,L}$ at $M_\infty=10$: \square , $C_x, H=0.25L$; \diamond , $C_x, H=0.5L$; \triangle , $C_x, H=0.75L$; \circ , $C_x, H=1.25L$; \blacksquare , $C_y, H=0.25L$; \blacklozenge , $C_y, H=0.5L$; \blacktriangle , $C_y, H=0.75L$; \bullet , $C_y, H=1.25L$; and \times , $C_{x,FM}$.

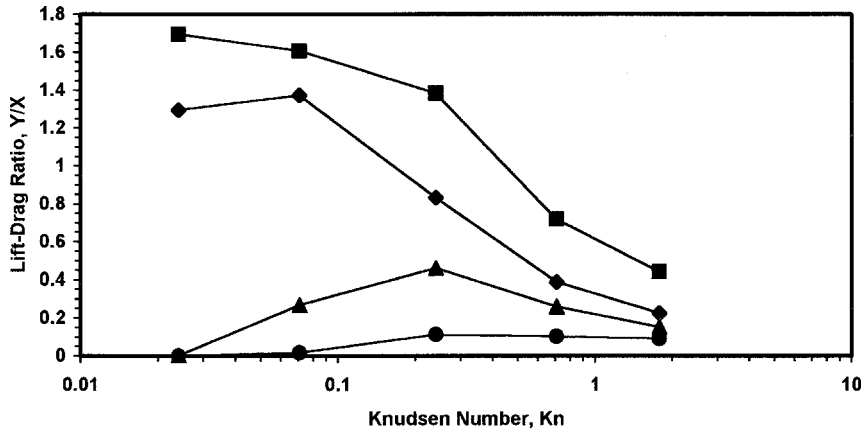


Fig. 13 Lift-drag ratio of the side-by-side plate vs Knudsen number $Kn_{\infty,L}$ at $M_\infty=10$: \blacksquare , $H=0.25L$; \blacklozenge , $H=0.5L$; \blacktriangle , $H=0.75L$; and \bullet , $H=1.25L$.

near side-by-side bodies. The rarefaction effects on the lift are significant even at large values of the geometric factor ($H/L=0.75$), and they are responsible for nonmonotonic dependency of the lift and lift-drag ratio on the rarefaction parameter of the Knudsen number at $1.25 \geq H/L \geq 0.25$. At large values of the Knudsen number $Kn_{\infty,L} \geq 1.8$, the drag correlates well with the drag value for the free-molecular flow¹⁴ (Fig. 12).

Conclusions

The hypersonic rarefied-gas flow about two side-by-side plates has been studied with the DSMC technique. The flow pattern and shock-wave shapes are significantly different for small and large

geometric ratios. At a value of the geometrical ratio parameter $H/L \leq 0.5$, the disturbances interact in the vicinity of the symmetry plane, creating a normal shock wave and a wide subsonic area, which occupies the whole “throat” area between the plates. This phenomenon affects the drag, pressure, and skin-friction distributions along the plates and produces significant repulsive lift force. A nonmonotonic dependency of lift, drag, and lift-drag ratio vs Knudsen number has been found for different geometric factors. The rarefaction effects on the lift force are significant at all considered values of the geometric factor $1.25 \geq H/L \geq 0.25$, and they are responsible for nonmonotonic dependency of the lift force and lift-drag ratio.

Acknowledgment

The author would like to express gratitude to G. A. Bird for the opportunity of using the DS2G computer program.

References

- ¹Koppenwallner, G., and Legge, H., "Drag of Bodies in Rarefied Hypersonic Flow," *Thermophysical Aspects of Reentry Flows*, edited by J. N. Moss and C. D. Scott, Vol. 103, Progress in Astronautics and Aeronautics, AIAA, Washington, DC, 1994, pp. 44–59.
- ²Bird, G. A., "Rarefied Hypersonic Flow Past a Slender Sharp Cone," *Proceedings of the 13th International Symposium on Rarefied Gas Dynamics*, edited by O. M. Belotserkovskii, M. N. Kogan, S. S. Kutateladze, and A. K. Rebrov, Vol. 1, Plenum, New York, 1985, pp. 349–356.
- ³Bird, G. A., *Molecular Gas Dynamics and the Direct Simulation of Gas Flows*, 1st ed., Oxford Univ. Press, Oxford, 1994, pp. 340–377.
- ⁴Gusev, V. N., Erofeev, A. I., Klimova, T. V., Perepukhov, V. A., Riabov, V. V., and Tolstykh, A. I., "Theoretical and Experimental Investigations of Flow Over Simple Shape Bodies by a Hypersonic Stream of Rarefied Gas," *Trudy TsAGI*, No. 1855, 1977, pp. 3–43 (in Russian).
- ⁵Riabov, V. V., "Comparative Similarity Analysis of Hypersonic Rarefied Gas Flows near Simple-Shape Bodies," *Journal of Spacecraft and Rockets*, Vol. 35, No. 4, 1998, pp. 424–433.
- ⁶Gorelov, S. L., and Erofeev, A. I., "Qualitative Features of a Rarefied Gas Flow About Simple Shape Bodies," *Proceedings of the 13th International Symposium on Rarefied Gas Dynamics*, edited by O. M. Belotserkovskii, M. N. Kogan, S. S. Kutateladze, and A. K. Rebrov, Vol. 1, Plenum, New York, 1985, pp. 515–521.
- ⁷Lengrand, J. C., Allège, J., Chpoun, A., and Raffin, M., "Rarefied Hypersonic Flow over a Sharp Flat Plate: Numerical and Experimental Results," *Rarefied Gas Dynamics: Space Science and Engineering*, edited by B. D. Shizdal and D. P. Weaver, Vol. 160, Progress in Astronautics and Aeronautics, AIAA, Washington, DC, 1994, pp. 276–284.
- ⁸Riabov, V. V., "Numerical Study of Hypersonic Rarefied-Gas Flows About a Torus," *Journal of Spacecraft and Rockets*, Vol. 36, No. 2, 1999, pp. 293–296.
- ⁹Coudeville, H., Trepaud, P., and Brun, E. A., "Drag Measurements in Slip and Transition Flow," *Proceedings of the 4th International Symposium on Rarefied Gas Dynamics*, edited by J. H. de Leeuw, Vol. 1, Academic Press, New York, 1965, pp. 444–466.
- ¹⁰Mavriplis, C., Ahn, J. C., and Goulard, R., "Heat Transfer and Flowfields in Short Microchannels Using Direct Simulation Monte Carlo," *Journal of Thermophysics and Heat Transfer*, Vol. 11, No. 4, 1997, pp. 489–496.
- ¹¹Oh, C. K., Oran, E. S., and Sinkovits, R. S., "Computations of High-Speed, High Knudsen Number Microchannel Flows," *Journal of Thermophysics and Heat Transfer*, Vol. 11, No. 4, 1997, pp. 497–505.
- ¹²Blevins, R. D., *Applied Fluid Dynamics Handbook*, Krieger, Malabar, FL, 1992, pp. 318–333.
- ¹³Bird, G. A., "The DS2G Program User's Guide, Version 3.2," G.A.B. Consulting Pty, Killara, NSW, Australia, 1999, pp. 1–56.
- ¹⁴Kogan, M. N., *Rarefied Gas Dynamics*, Plenum, New York, 1969, pp. 345–390.

I. D. Boyd
Associate Editor